Japan Geoscience Union Meeting 2015
(May 24th - 28th at Makuhari, Chiba, Japan)

SSS30-P01 Room:Convention Hall Time:May 25 18:15-19:30

Two seamounts in the near south of Nankai Trough concentrate stress like stake

MASE, Hirofumi[1*]

[1]none

(Please refer to the figure. Names of the slab, topography of seabed, etc are naming only of here.)

Collapse by intraplate earthquake, Separation of accretionary wedge, and Rotation of Slab by lateral-fault type are Nankai-Trough earthquakes. The role of the 2004 off Kii Peninsula earthquake is the settlement of the 1944 Tonankai earthquake (1). I want to search for the relation of both earthquakes further. I post almost clear points by (1)-(5).

(A):Concerning range of slip, it of 1944 did not reach the Trough, and it of 2004 twined round the Trough. Both are complementary and do not overlap so much.

(the following points are concerned in 2004)(B):The compression power in north-south is the cause.

(C):The foreshock, the main shock, and big aftershocks are distributed along the Trough, and are almost thrust-type that destroyed intraslab.

(D):Aftershocks distributed in northwest-southeast are almost shallow and lateral-type. In the accretionary wedge and the upper layer-of-lower-plate, the large-scale lateral fault belt exists.

(E):Everything is distributed in the west of the Crack(b).

(F):On the extension of the south end of the Crack(a), two big thrust-type aftershocks in 2 or 3 days occurred after the main shock.

(G):Large slip of the foreshock was in the deep place and in the vicinity of the hypocenter. That of the main shock was in the shallow place and in the west left from the hypocenter.(3) After all, the positions of both large slip are near.

About the large slip(G), there is Daiozaki Cape in almost due north and is WM Seamount in south. I think that the compression power(B) was the maximum in this north-south line. So that the power from the north that originates in the right-turning force(1) may concentrate in a narrow range in the vicinity of the Trough, existence like stake that concentrates the stress of reaction is dynamically indispensable in the south nearly of the Trough. WM Seamount might be ”Stake” exactly. EM Seamount where aftershock(F) occurred shortly in the vicinity might be ”Stake” too. The lateral fault belt(D) passes between two ”Stakes” in east and west.

The stress of WM Seamount that was large before the earthquake decreased sharply by the large slip(G). At this point, the north-south compression(B) has collapsed. Next, what happens? Because materials that exist in the left above of both ”Stake” in Fig.2 are alive and well, the stress from that direction(northwest) increases rapidly.

In a word in 2004, the north-south compression after 1944(B) might have been converted to the northwest-southeast compression in dramatic form. And, there is naturally a possibility of returning to the north-south compression(B) again in the future. Only this is the Tonankai earthquake when the future. Only this was the Tonankai earthquake in 1944.

(1)MASE(2014)/JpGU2014/SSS29-P10

(2)YAMANAKA(2004)/Source rupture processes of the 1944 Tonankai earthquake and the 1945 Mikawa earthquake/Chikyu Monthly/26/11/739-745

(3)YAGI(2004)/http://iisee.kenken.go.jp/staff/yagi/eq/Japan20040905/Japan20040905_1-j.html

(4)JMA/Monthly Report/September 2004

(5)KANAZAWA/http://cais.gsi.go.jp/YOCHIREN/history/2-3-6_kii2004.pdf

SSS30-P01 Room:Convention Hall Time:May 25 18:15-19:30

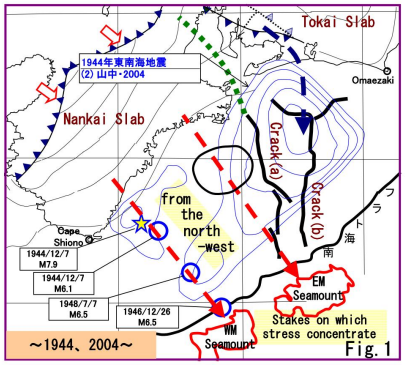

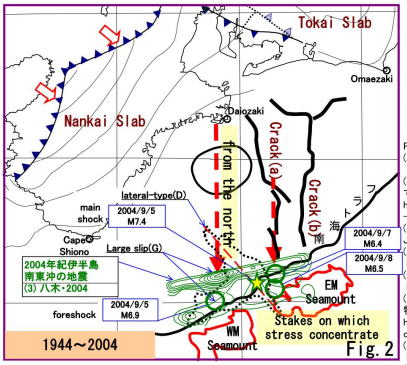

/About sea bottom
(shape line)
extracted from (6)/
/About "Nankai Slab"
(shape line, contour)
referable to (7)/
/About "Tokai Slab"
(shape line, contour)
referable to (8)/
/About information on earthquake
(All not mentioned specially)
referable to (9)/

Reference literature
(2)山中佳子(2004)/1944年東南海地震と1945年三河地震の震源過程
/月刊地球/26/11/739-745
(3)八木勇治(2004)/2004年9月5日紀伊半島南東沖で発生した地震について/建築研
http://iisee.kenken.go.jp/staff/yagi/eq/Japan20040905/Japan20040905_1-j.html
(4)JMA/Monthly Report on Earthquakes and Volcanoes in Japan/September 2004/特集2/図6-5(P64)等
(5)金沢敏彦/紀伊半島沖[三重県南東沖]の地震/東大震研
http://cais.gsi.go.jp/YOCHIREN/history/2-3-6_kii2004.pdf
(6)JHOD,JCG/Seafloor Topography of the Plate Boundaries
http://www1.kaiho.mlit.go.jp/jishin/sokuryo_E/sokuryo_E.html
(7)木村昌三(2001)/1946年南海地震に関係する四国における地震活動の特徴/(図2)
https://www.jstage.jst.go.jp/article/jgeography1889/110/4/110_4_581/_article/-char/ja/
(8)Nagoya Univ./Structure of the Subducting Philippine Sea Slab
http://www.seis.nagoya-u.ac.jp/SEIS/slab/slab-j.html
(9)JMA/Monthly Report on Earthquakes and Volcanoes in Japan/September 2004/特集2/図7-1(P65)
http://www.seisvol.kishou.go.jp/eq/gaikyo/index.html#monthly

Japan Geoscience Union Meeting 2015
(May 24th - 28th at Makuhari, Chiba, Japan)

SSS30-P02 Room:Convention Hall Time:May 25 18:15-19:30

Toward rapid source process analysis for great earthquake using teleseismic body waves

YOSHIMOTO, Masahiro[1*] ; YAMANAKA, Yoshiko[1]

[1]Environmental studies, Nagoya University

Source processes for great earthquakes are now obtained in near-real-time by teleseismic body wave analyses. Green's functions of most teleseismic body waves analyses are based on ray theoretical method, but such methods have the following two problems for great earthquakes source process analyses: difficulty in calculating all later phases such as PP waves and impossibility of calculating very long period phase called a W phase. To solve these problems, we introduced the complete Green's functions (i.e., all body and surface waves) calculated by Direct Solution Method. We show that source process analyses results of 2011 Tohoku-Oki earthquake (Mw7.3), 2007 Solomon earthquake (Mw8.1), and 2010 Chile earthquake (Mw8.8) using the complete Green's functions. We also analyzed these earthquakes using the conventional ray theoretical Green's functions in order to make clear the problems of ray theoretical method. The obtained 2011 Tohoku-Oki earthquake source process using complete Green's functions is not so different from ray theoretical Green's functions. However, the source process of 2007 Solomon and 2010 Chile earthquake using conventional ray theoretical Green's functions are quite different especially later part of source process compared with that of using the complete Green's functions. These difference mainly caused by neglecting W phase of the ray theoretical Green's functions calculation. When you analyze the great earthquake in near-real-time using ray theoretical Green's functions, we recommend that you should be use the station of small amplitude W phase as much as possible and may be better use velocity observed seismograms rather than displacement observed seismograms.

Keywords: teleseismic body waves, Green's functions, ray theory, W phase, great earthquake

Japan Geoscience Union Meeting 2015
(May 24th - 28th at Makuhari, Chiba, Japan)

SSS30-P03 Room:Convention Hall Time:May 25 18:15-19:30

Optimization of Preset Parameters for Source Process Analysis with Teleseismic Body-Wave

FUJITA, Kenichi[1*] ; KATSUMATA, Akio[1] ; SAKODA, Koji[2] ; SHIMIZU, Jumpei[2] ; HASEGAWA, Yoshiomi[2]

[1]Meteorological Research Institute, [2]Japan Meteorological Agency

1. INTRODUCTION

The Japan Meteorological Agency (JMA) analyzes source process of earthquakes in the world larger than Mw7.0 with teleseismic body-wave. The results are published on the website. It is generally difficult to determine optimum preset parameters for source process analysis, because there are so many parameters for the analysis. Therefore, it takes a long time until publish the results.

We examined optimized preset parameters to automate source process analysis with teleseismic body-wave. Here, we analyze some events using parameters which are determined automatically, and compare them with the results which were analyzed through trial and error by the analyst. Then, we extract problems which arises in automatic parameter determination and seek the solutions.

2. Methods

We use the same program package as Iwakiri et al. (2014) for analyzing source process with teleseismic body-wave. We use broadband waveform data which are downloaded from IRIS DMC HP, and apply band-pass filter (from 0.002Hz to 0.125Hz) to them. We use epicenter data of JMA for events in and around Japan, we use epicenter data of USGS for events in other areas. We use depth of CMT solutions of JMA for the depth of starting point. Hypocenter is set at center of assumed fault plane, and subfault parameters (size and number) are set by scaling law. Strike, dip and rake parameters are set from CMT solutions of JMA. Velocity structure for Green's functions are set based on the IASP91 model, and CRUST2.0 model for near hypocenter. Source-time functions are set with triangle functions. The number of function is changed based on event magnitude. And rise time is set at 2.0sec. We use ABIC (Akaike (1980)) for temporal and spatial smoothing constraints, and set hyperparameters as ABIC value become the minimum. Max rupture speed is set at 0.72 times of S-wave velocity from empirical relationship of Geller (1976).

Keywords: source process, optimized preset parameters, automation

Japan Geoscience Union Meeting 2015
(May 24th - 28th at Makuhari, Chiba, Japan)

SSS30-P04 Room:Convention Hall Time:May 25 18:15-19:30

Consideration of the Method to Estimate the Radiated Seismic Energy from Regional Seismic Waveforms

KIUCHI, Ryota[1*] ; MORI, James[1]

[1]DPRI, Kyoto University

The total released strain energy during an earthquake is divided into frictional energy, fracture energy, and radiated seismic energy. In these 3 components, we can estimate only the radiated seismic energy directly from the seismic waveform, and that characterizes the dynamic source property. There are large variations of radiated seismic energy from previous energy estimate studies, although it is difficult to estimate it due to the contribution from a wide frequency spectrum. One of the probable factors of this variation is focal mechanism dependence of radiated seismic energy from teleseismic waveforms (e.g., Choy and Boatwright, 1995; Convers and Newman, 2011). However, there are 2 additional questions from these studies. 1. These results were obtained only from P wave energy assuming a ratio between P wave energy and S wave energy. Teleseimic S waves often overlap with other phases, and attenuate more strongly than P waves, so it is difficult to measure the S-wave energy directly. The ratio of P to S radiated energy is not well known. 2. The focal mechanism dependence has been shown only for large earthquakes (Mw >6), it seems that this characteristic has not been observed for small and moderate earthquakes.

For the purpose of investigating these questions, we need to estimate and compare the radiated seismic energies correctly from several different phases. As an example, we focus on a moderate earthquake (June 14, 2008 at 12:27, Mw 4.9 from F-net) that occurred just after 2008 Iwate-Miyagi Nairiku earthquake. In this study we estimate the radiated seismic energy from regional P waves, S waves, and S wave coda using an empirical Green's function (EGF) method. The regional waveform data are recorded at stations of Hi-net. Firstly, using cross correlation, we select an EGF event that is highly correlated with the target event. Secondly, we deconvolve the seismograms in frequency domain with a multitaper method (Prieto et al., 2009), and check the waveform in time domain. Thirdly, we fit the obtained spectrum to an omega square model (Brune, 1970, 1971) to estimate the corner frequency. In addition, we try to vary the value of the power for the high-frequency fall-off. Finally, we calculate the radiated seismic energy using these spectra.

Acknowledgement
The regional waveform data of Hi-net and focal mechanisms of F-net were provided by NIED.

Keywords: Seismic radiated energy, Moderate earthquake

Japan Geoscience Union Meeting 2015
(May 24th - 28th at Makuhari, Chiba, Japan)

SSS30-P05 Room:Convention Hall Time:May 25 18:15-19:30

Simulation of hypocenter determination by using S-net stations

SHIMBO, Takashi[1*] ; UEHIRA, Kenji[1] ; KANAZAWA, Toshihiko[1] ; MOCHIZUKI, Masashi[1] ; FUJIMOTO, Hiromi[1] ; NOGUCHI, Shin-ichi[1] ; KUNUGI, Takashi[1] ; SHIOMI, Katsuhiko[1] ; AOI, Shin[1] ; SEKIGUCHI, Shoji[1] ; MATSUMOTO, Takumi[1] ; OKADA, Yoshimitsu[1] ; SHINOHARA, Masanao[2] ; YAMADA, Tomoaki[2]

[1]NIED, [2]ERI

To observe earthquakes occurring under seafloor and tsunami, project to construct Seafloor Observation Network for Earthquakes and Tsunamis along the Japan Trench (S-net) is started in 2011. The S-net consists of 150 seismic and tsunami observation stations. These stations are arrayed from off Hokkaido to off Boso at intervals of about 30km in the direction North-South (parallel to the trench axis) and at interval of about 50-60km in the direction East-West (perpendicular to the trench axis). S-net makes it possible to forecast earthquake warning and tsunami warning much earlier than presence. To understand occurrence of earthquake occurring under seafloor, we must research hypocenters distribution, focal mechanism, velocity structure, and stress field under seafloor accurately. Then we need to research relationship between subducting plate and occurrence of earthquake and process of strain accumulation at interplate. To research these in detail, we need to locate hypocenters under seafloor precisely.

To understand accuracy of hypocenters determined by S-net, we simulated of hypocenter determination by using travel times from earthquake occurring under seafloor to stations of S-net. 99 aftershocks at the southern region of 2011 off Pacific Cast of Tohoku Earthquake located by pop-up ocean bottom seismometers (OBSs) (Shinohara et al., 2011) were used. We calculated travel times from these hypocenters to S-net stations and estimated arrival times of every station. Hypocenters were determined by using the arrival times. Then velocity structure used calculation of travel times and determination of hypocenters was modeled by introducing result of seismic survey for installation of S-net. We compared hypocenters located by simulation of this study with those located by OBS data (Shinohara et al., 2011). As the result, difference in the hypocenters was about 1km. We run same simulation by using Hi-net land stations. Then velocity structure used calculation of travel times and relocation of hypocenters was velocity model used determination of hypocenter in Kanto and Tokai area (Ukawa et al., 1984). As the result, several hypocenters by simulation of this study were determined 5km deeper than those by OBS. This indicates that determination of hypocenter using only land seismic stations is not sufficiently precise.

Japan Geoscience Union Meeting 2015
(May 24th - 28th at Makuhari, Chiba, Japan)

SSS30-P06 Room:Convention Hall Time:May 25 18:15-19:30

The M 7.7 September 24, 2013 Pakistan earthquake: comparison of back-projection images and field data

WANG, Dun[1*] ; MORI, James[2] ; KAWAKATSU, Hitoshi[1]

[1]Earthquake Research Institute, The University of Tokyo, [2]Disaster Prevention Research Institute, Kyoto University

We analyzed the 24 September 2013 Pakistan earthquake (Mw 7.7) by back-projecting seismograms recorded by several large regional arrays in Japan, China, and Europe. The results show that the rupture propagated towards the southwest, and released most of the high frequency energy at 90-130 km southwest of the epicenter around 20-40 s after the initiation. This rupture pattern is significantly different from the northward propagation which would have been expected from the aftershock distribution.

High frequency images suggest that the average rupture speed is 4.0 to 5.0 km/s. The rupture speed seems relatively slow (1.0 to 2.0 km/s) for the first 10-15s, and then increased to fast, possibly supershear (4.0 to 6.0 km/s). Relatively lower frequency images show a lower rupture speed of 3.0 to 3.5 km/s (Figure 1).

A comparison of rupture traces determined by the back-projection and a geodetic study provides a good test for resolution of the back-projection method. Given a correct epicenter location, results derived from seismograms recorded in Hi-net, show a very accurate location of the surface trace with an uncertainty of 10-20 km.

Figure caption

Figure 1 Timings and amplitudes for the stack with the maximum correlation at each time step (1 s) showing in the map (top) and as a function of time derived from data recorded in Europe, China, and Japan (from left to right) filtered in several high frequency bands (bottom). Here the distance is measured in a straight line from the relocated epicenter.

Keywords: source process, back-projection, slip model, rupture speed

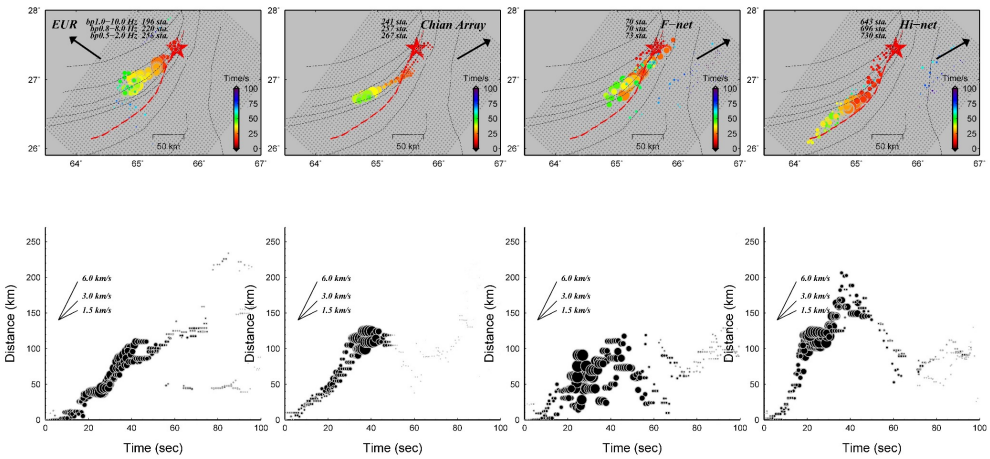

Japan Geoscience Union Meeting 2015
(May 24th - 28th at Makuhari, Chiba, Japan)

SSS30-P07 Room:Convention Hall Time:May 25 18:15-19:30

Source process analysis of the 1923 Kanto earthquake using 3-D Green's functions and a curved fault model

YUN, Sunhe[1*] ; KOKETSU, Kazuki[2] ; KOBAYASHI, Reiji[3]

[1]Earthquake Research Institute,The University of Tokyo/Itochu techno-solutions, [2]Earthquake Research Institute,The University of Tokyo, [3]Graduate School of Science and Engineering, Kagoshima University

The Kanto earthquake occurred on September 1, 1923 (UTC). The source region included the land area, causing severe damage in the Kanto district. This is an inter-plate earthquake along the Sagami trough. Large seismic intensities were observed not only around the source region but also in areas far from there. This strange distribution was caused by a 3-D complex structure of the Kanto basin. We calculated Green's functions using a Japan integrated velocity structure model by Koketsu et al. (2008) to include effects of the Kanto basin on ground motions and we performed source process inversions of the Kanto earthquake. This model reflects a 3-D complex shape of the Kanto basin and sedimentary layers are more than 3 km under the Tokyo bay and the northern Chiba prefecture. The dataset consists of static displacement, teleseismic, and strong motion data. We adopted both the same fault model as used by Sato et al. (2005) and a curved fault model. For the latter model we reconfigured the depths following the plate boundary.

We first calculated Green's functions using a half-space medium, a 1-D and a 3-D velocity structure model. The 3-D Green's functions are larger and longer than others and amplified later phases are remarkable. This means soft and 3-D complex sedimentary layers amplify Green's functions. We performed source process inversions using these Green's functions and geodetic data. All results show the similar large slip areas. But the total seismic moment of the result using 3-D Green's functions is the smallest. This implies amplifications by the basin also affect source process inversion results of only geodetic data. Next we used 3-D Green's functions and performed a joint inversion of static displacement, teleseismic, and strong motion data with the plane fault model. The large slip areas are similar to the result of Sato et al. (2005) but our result shows smaller slips and a smaller total seismic moment. In addition, we could obtain inversion results that provide good agreement in the later parts of the strong motions. We finally used 3-D Green's functions and performed a joint inversion with the curved fault model. The results show the western large slip area is moved to the southwest on the shallow part of the plate boundary, where is far from the hypocenter. Our result with the curved fault model shows larger slips and a larger total seismic moment than our result with the plain fault model. This is because the depths of the curved fault model are deeper, so Green's functions are smaller.

The results by the plane fault model and Sato et al. (2005) obtained the western large slip area where many aftershocks occurred. But our result with the curved fault model obtained the western large slip area where relatively a few aftershocks occurred. This is coincident with previous researches about the relationship between slip distributions and aftershock distributions. On the other hand, both the results with the plane and curved fault models show similar rupture propagations. The rupture started at a protruded area on the plate boundary and propagated to shallow southern parts for the initial 20 s. Then the rupture propagated to eastern areas where the plate boundary is dented for the next 20 s.

This study indicates that a velocity structure should affect not only strong motions but also static displacements for earthquakes occurred beneath the Kanto basin, which has thick sedimentary layers and a 3-D complex velocity structure. As a result, source process inversion results using a half-space and 1-D velocity structure models may overestimate slips and total seismic moments. In addition, we could obtain inversion results that provide good agreement with strong motions. This indicates the significance of using 3-D Green's functions in source process inversions. And the result with the curved fault model shows the slip distribution agrees with the established theory on aftershock patterns and a main shock faulting.

Keywords: source process inversion, 3-D Green's function, Kanto basin

Japan Geoscience Union Meeting 2015
(May 24th - 28th at Makuhari, Chiba, Japan)

SSS30-P08 Room:Convention Hall Time:May 25 18:15-19:30

Reproduction of M˜2 earthquakes by elastic Boundary Element modelling and constraint of Mohr-Coulomb failure criterion

UCHIURA, Taka[1*] ; HOFMANN, Gerhard[2] ; WIGGINS, Mitch[3] ; STONE, Wouter[3] ; NDABA, Pinkie[3] ; PLOTZ, Janelle[3] ; LENEGAN, Patrick[3] ; YILMAZ, Halil[4] ; ZVARIVADZA, Tawanda[4] ; MNGADI, Siyanda[4] ; CARPEDE, Andrew[4] ; DURRHEIM, Raymond[5] ; MILEV, Alexv[6] ; OGASAWARA, Hiroshi[7] ; YABE, Yasuo[8] ; KATO, Harumi[9]

[1]Ritsumeikan University, [2]Anglogold Ashanti, [3]Sibanye Gold, [4]Witwatersrand University, [5]CSIR / Witwatersrand University / SATREPS, [6]CSIR, [7]Ritsumeikan University / SATREPS, [8]Tohoku University / SATREPS, [9]3D Geoscience, Inc.

Several M˜2 earthquakes have taken place at a mine, close to one of the sites of the JST-JICA SATREPS project. At this site, three Ishii borehole strainmeters were installed, continuously monitoring at a sampling frequency of 100Hz since December 2011 and achieving better data return than previous projects. Although an AE network was not planned at this site, CSIR installed four 14Hz geophones with spatial intervals less than 100m to improve hypocenter location accuracy of the in-mine seismic network (station intervals $>$˜500m yielding a few ten of meters of errors in epicenter locations and much larger errors in z-location). The initial stress assumption was well calibrated at the adjacent mine (˜3 km to the west; Hofmann et al., 2013) and in-situ stress measurements ˜1km to the south in a mine are available. Uniaxial laboratory tests were conducted to measure elastic and strength properties of selected core collected from the nine holes with a total length of about 340 m for the instrumentation,.

This study attempted to numerically simulate four M˜2 earthquakes (one and the next occurred in December 2013 and January 2014 respectively and the remaining two in August 2014) that occurred in a range of distances from 180m to 351 m from the site by using an elastic Boundary Element stress modelling software, Map3D. In Map3D stress modelling, non-linear elasto-plastic fault ride is reproduced with its magnitude and extent controlled by the peak and residual strength, when estimated stress reaches specified peak strength.

Hofmann et al. (2012) successfully reproduced plausible source size and mechanism of an Mw2.2 event which had occurred at a dyke at Mponeng mine in December 2007. They took into account the aftershock planer cluster Yabe et al. (2009) delineated by the JAGUARS AE network (Nakatani et al., 2008). Hofmann et al. found that the aftershock plane coincided with that plane with largest Excess Shear Stress (i.e. shear stress exceeding shear strength; ESS). It could therefore be suggested that we could define slip planes with some confidence if we find planes with maximum ESS.

In this study, progressive tabular mining about 1m thick was modelled on a mine-wide scale by Displacement Discontinuity planes that represented the monthly advance of mining faces from December 2012 to August 2014. We used the initial stress state determined by Hofmann et al. (2013) and calibrated with several in-situ stress measurements in adjacent mines several km to the west of a mine. We also confirmed the assumed initial stress could reproduce stress states capable of producing breakout or core-discing that was actually observed in nine instrumental holes at our site. In the stress states just prior to the occurrence of the four M˜2 events, we grid-searched (in 10 degree increments of dip) for the plane with maximum ESS that contained the located hypocenter and had a strike parallel to the edge of the closest thin tabular stope. We found that for three of the four M˜2 event, composite plots of shear stress versus normal stress on assumed fault planes were relatively well limited by a single Mohr-Coulomb strength criterion line, but the strength suggested was significantly larger than those suggested by Hofmann et al. (2012), while the strength suggested for the remaining event were similar to that estimated by Hofmann et al. (2012). We have to discuss potential reasons, e.g., alteration of stress field by some geological structures or difference between intact rock and existing plane of weakness. The progress in the discussion, including analyses of the monitored strain change, will be reported in 2015 JpGU meeting.

Keywords: Mohr-Coulomb failure criterion, Deep South African mines, Elastic Boundary Element modelling, Stress in seismogenic zone

Japan Geoscience Union Meeting 2015
(May 24th - 28th at Makuhari, Chiba, Japan)

SSS30-P09 Room:Convention Hall Time:May 25 18:15-19:30

Detection state of stress at a fault from focal mechanism data ? application to Kego fault-

MATSUMOTO, Satoshi[1*] ; MIYAZAKI, Masahiro[1] ; SHIMIZU, Hiroshi[1]

[1]Institute of Seismology and Volcanology, Kyushu Univ.

One of the approaches used to evaluate the potential of an earthquake occurrence is the detection of the stress concentration at an earthquake fault. The stress fields for pre- and post-seismic event stages differ. However, this change cannot provide information regarding the potential for an earthquake to occur. Matsumoto et al. (2014) have proposed a detection method for states of stress that uses focal mechanism data of microearthquakes. The state of stress in this study can be defined by a moment tensor equivalent to the stress concentration normalized by differential stress. We apply this method to actual focal mechanism data from the 2005 Fukuoka earthquake and around the Kego fault, Kyushu, Japan, and discuss the presence of stress concentration around the earthquake fault before the mainshock.

Keywords: stress field, state of stress, focal mechanism, Kego fault

Japan Geoscience Union Meeting 2015
(May 24th - 28th at Makuhari, Chiba, Japan)

SSS30-P10 Room:Convention Hall Time:May 25 18:15-19:30

Estimates of stress drop in the focal area of the 2008 Iwate-Miyagi nairiku earthquake

YOSHIDA, Keisuke[1*] ; HASEGAWA, Akira[2] ; OKADA, Tomomi[2] ; UCHIDA, Naoki[2]

[1]National Research Institute for Earth Science and Disaster Prevention, [2]Tohoku University

Earthquakes release the deviatoric stress in the earth by slip on faults. We can estimate the magnitudes of the shear stress reductions (stress drops) on the faults through frequency analysis of seismic wave. Stress drop is an important parameter in earthquake cycle. However, it is generally difficult to accurately determine the stress drop. This is because it depends on many assumptions, and the estimates are largely affected by the errors of the corner frequency. Therefore, meanings of stress drop variations are not well understood. One possibility is that stress drops may related to frictional strengths on the fault planes. Determinations of absolute frictional strengths are very difficult. However, we can estimate the relative strengths from fault plane orientations of focal mechanisms in homogeneous stress regions. In this study, we investigate the relationship between stress drop and frictional strength. For that, we apply a multi-window spectral ratio method of Imanishi and Ellsworth [2006] to data from the dense aftershock observation network in the aftershock area of the 2008 Iwate-Miyagi nairiku earthquake. In the focal area, the stress orientations were estimated by Yoshida et al. [2014a and b]. Furthermore, the deviatoric stress tensors in the focal area were also estimated based on the rotations of principal stress axis after the mainshock [Yoshida et al., 2014b].

We estimated stress drops for earthquakes listed in JMA catalogue with magnitudes greater than 1.0. First, velocity spectrums of S-wave were calculated for three time windows, whose lengths are 2s moving in steps of 1s from 0.2s before the S-wave arrivals. Also, the velocity spectrums of noise were computed from time windows before the P-wave arrivals. We omitted data with S/N $<$5.0 near their expected corner frequencies. Second, spectral ratios were calculated between events within 1 km. For the hypocenters, we adopted those determined by double-difference methods to arrival time data from the temporary stations above the focal area [Yoshida et al.,2014b]. Third, corner frequencies were estimated by fitting the stacked spectral ratios with omega-square source model by Boatwright [1978]. Again, we omitted the results for which we could not constrain the corner frequencies enough due to high residuals. Finally, we estimated the stress drops using the circular crack model of Sato and Hirasawa [1973] and Eshelby [1957].

The number of estimated stress drops was 761. The mean and median values are 5.1 and 4.5 MPa, respectively. Although estimated values of them scatter, we found a positive correlation between the stress drop and the focal depth. For comparisons with frictional strengths, we estimated the relative frictional strengths based on the four stress orientations estimated by Yoshida et al. [2014a and b] in various spatial scales. For the estimations, we assumed the uniform differential stress magnitude within the focal area. In all cases, we see the positive correlation between the stress drops and the relative frictional strengths. In addition, we compared the results with the absolute frictional strengths estimated by Yoshida et al. [2014b] based on the spatially variable deviatoric stress tensors. Again, we found a positive correlation of the stress drops with the frictional strengths. These suggest that static stress drop released by earthquakes is related to the absolute stress level on fault plane.

Keywords: stress drop, stress tensor inversion, frictional strength, focal mechanism

Japan Geoscience Union Meeting 2015
(May 24th - 28th at Makuhari, Chiba, Japan)

SSS30-P11 Room:Convention Hall Time:May 25 18:15-19:30

Deep tremors response to tidal stress in western Japan: Analysis by Schuster's test

KIKUCHI, Junji[1*] ; YABE, Suguru[1] ; IDE, Satoshi[1] ; TANAKA, Yoshiyuki[2]

[1]Department of Earth and Planetary Scinence, The University of Tokyo, [2]Earthquake Reserch Institute, The University of Tokyo

In Japan, many deep tectonic tremors occur in the Nankai subduction zone from the center of Honshu to western Shikoku. Each tremor is a tiny shear slip that reflects local plate motion. Thus the physical conditions that enhance tremor activity would also control plate motion to some extent. For example, in a small tremor cluster beneath south Okayama, tremor rate is extremely well correlated with tidal level [Ide & Tanaka, 2014]. Here, we calculate ocean and solid earth tidal stress on the plate interface and quantitatively evaluate the degree of tidal triggering of tremors in the Shikoku region using the Schuster's test [e.g., Tsuruoka et al.,1995].

In the Shikoku region, we calculate normal and shear stresses at each reference point located at 0.1^o interval at 30 km depth, assuming a low-angle thrust fault based on global subducting plate motion. We compute the spatial distribution of theoretical ocean height using NAO.99b [Matsumoto et al., 2000] and convolve it with Green's function [Okubo & Tsuji, 2000] to obtain an ocean tidal stress tensor. We also calculate a stress tensor by solid earth tide using tide-generating potential of Tamura [1987]. The tremor catalog is of Idehara et al. [2014], for the nine years period from April 1, 2004 to March 31, 2013. We use tremors within $\pm 0.1^o$ in latitude and longitude, respectively, from each reference point.

In the Schuster's test, a phase angle of 0^o is assigned to the maximum stress peak nearest to the tremor occurrence time and $\pm 180^o$ to the following and preceding minima respectively. Based on the phase angles of all tremors, we calculate the significance level p for rejecting the null hypothesis that tremors occur randomly, regardless of stress. In general, small p means large statistical significance, and p less than 1% is considered significant in many previous studies.

We found some spatial variation in tremors response to tide. For example, in Kagawa, we found that two tremor clusters of similar sizes separated by 20km differently respond to tidal stress. The western cluster shows a strong tidal dependency (p=7.6e-44%), while eastern cluster has two peaks in phase angle and its tidal dependency is obscure. By changing fault parameters for the east cluster, we found that a low p (=0.7%) and a single peak in phase angle are obtained with some mechanisms similar to strike slip. This result implies that fault structure in Eastern Shikoku is complex and that tremor occurring mechanism changes locally.

Keywords: deep tectonic tremors, tide, Schuster's test, Nankai Trough, Shikoku

Japan Geoscience Union Meeting 2015
(May 24th - 28th at Makuhari, Chiba, Japan)

SSS30-P12 Room:Convention Hall Time:May 25 18:15-19:30

Seismicity Activation around the Kurobe Dam Reservoir in Oct. 2011

SATO, Takanobu[1*] ; KIM, Ahyi[1] ; OHMI, Shiro[2]

[1]Yokohama City University, [2]Disaster Prevention Research Institute, Kyoto University

After the March 2011 Tohoku-Oki earthquake, seismicity activation was observed wide range of beneath the Hida mountain area. However, another significant seismicity occurred around the Kurobe dam reservoir in October 2011. It was initiated by M3.9 earthquake followed by two magnitude larger than 5.0 quakes and the activity lasted for a couple of weeks. No active earthquake faults have been recognized, and no significant seismic activities or magnitude larger than 5 events have been observed previously except the ones observed in 1960s due to filling of the reservoir. The question is if the seismicity observed in October 2011 was related to the dam reservoir. To address question, we will examine the stress state of the area before and after the seismicity. As a first step of the study, we relocated 222 earthquakes observed in this area from Mach to November 2011. Then we analyzed 24 focal mechanisms to etch the shape of fault line. The results showed the epicenters moved 1.5 km eastward and two major faults, one with strike between 160 and 175 degrees, and another with strike between 180 and 195 degrees, were illuminated. Next we calculate the Coulomb failure function(ΔCFF) if the seismicity can be explained by static stress change due to the seismic activity occurred in March. The results indicate that although M5.4 and M5.2 events were possibly triggered by M3.9 and M5.4 events respectively, and the successive aftershocks were triggered by both M5.4 and M5.2 events, It might be difficult to trigger M3.9 earthquake just because of the static stress change due to the seismicity in March 2011. To figure out other causes which can trigger M3.9 event, we examined a dynamic stress triggering and found there was about 8kPa dynamic stress change due to a remote earthquake. As the next step, we will examine if there is any significant pore pressure change so that the seismicity can be triggered by such a small stress change.

Keywords: Seismic activity, Coulomb failure stress change, Dynamic stress change, Pore water pressure, Shear wave anistropy, Hida mountains

Japan Geoscience Union Meeting 2015
(May 24th - 28th at Makuhari, Chiba, Japan)

SSS30-P13 Room:Convention Hall Time:May 25 18:15-19:30

Development of the quasi-dynamic cycle simulation code including both great and small earthquakes

TAKASAKI, Keisuke[1*] ; HIRAHARA, Kazuro[1] ; OHTANI, Makiko[1]

[1]Graduate School of Science,Kyoto University

The magnitude-frequency relation of earthquakes is formulated as Gutenberg-Richter law (GR law). The b values in the GR law take different ones depending on the regions and also show temporal changes. If the b value increases,the number of large earthquakes relatively decreases,and vise versa.

Nanjo et al.(2012) reported that the b value had decreased during a period of ten years before great earthquakes,such as 2011 Tohoku and 2004 Sumatra earthquakes. They suggested that the decrease of the b value can be phenomenon before the occurrences of great earthquakes.

Tormann et al.(2015) reported that the b value,which increase after the 2011 Tohoku earthquake,decreased to the value nearly equal to that before the earthquake.

Although the physical mechanism of the temporal change in the b value has remained unclear,small but many earthquakes may give some effect on the occurrence of great earthquakes or at least the change in the b value can be an indicator of stress state in the focal regions of great earthquakes. It may lead to forcasting great earthquakes that we understand the physical mechanism of the temporal change in the b value. One of ways for clarifying the physical mechanism is to simulate earthquake cycles,which include not only great earthquakes but also small ones,and reproduce the spatio-temporal change in b value for a variety of rate- and state friction models.

Since interseismic period is much longer than coseismic one,the adaptive time-step control Runge-Kutta method is usually used in the present simulations. While the time-steps take small values around the coseismic period with large slip rates,the time-steps take larger ones in the interseismic period with smaller slip rates. Most of present simulations reproduce only great earthquakes,not including many earthquakes with different magnitudes.

If the small earthquakes whose magnitude-frequency relation obeys the GR laws are simulated in addition to great ones,the earthquakes always occur and requires small time-steps in the whole period,leading to the huge computational costs. Thus,we have to reduce the costs for small earthquake simulations in particular to realize the realistic cycle simulations of earthquakes with a variety of sizes.

As noted above,it is the key issue to reduce the computational costs in order to simulate the spatio-temporal change in the b value in the focal region during great earthquake cycles. In our simulations,we use the boundary element method and the quasi-dynamic approximation(Rice,1993).

In addition to the problem of time-steps,the time consuming part is the product calculation of the slip response function matrix and the slip velocity vector. When plate interface is divided into the N small subfaults, the computational cost is O($N*N$). N become much larger when including small earthquakes. We apply H-matrices method to the product part in cycle simulations,which reduces the memory size and the CPU time to O(N)-O($N\log N$)(Ohtani et al.,2011).

As described above,we have to use small time-steps in cycle simulations including also cycles of many small earthquakes,and the computational costs become huge. For this reason,RSQSim(Dieterich and Richards-Dinger,2010) code has been developed. In this study,however,we try to develop another code which performs the same quasi-dynamic cycle simulations for large earthquakes as in the usual ones and the simplified ones for small earthquakes. Namely,when the stress at a patch of small earthquake reaches a certain value,the stress is released and the slip and slip velocity are given in proportion to the stress drop.

In the talk,we give some details of the computation and evaluate our model. Furthermore,we add discussion on the current problems and th future perspectives of our approach.

Keywords: earthquake cycle, numerical simulation, Gutenberg-Richter law, fast computation

Japan Geoscience Union Meeting 2015
(May 24th - 28th at Makuhari, Chiba, Japan)

SSS30-P14 Room:Convention Hall Time:May 25 18:15-19:30

Recurrence intervals of Miyagi-oki earthquakes after the 2011 Tohoku-oki earthquake based on numerical simulations (II)

NAKATA, Ryoko[1*] ; ARIYOSHI, Keisuke[1] ; HYODO, Mamoru[1] ; HORI, Takane[1]

[1]JAMSTEC

Along the Japan Trench, interplate earthquakes (M7.1-7.4), which described as Miyagi-Oki earthquakes have occurred with recurrence intervals of approximately 30-40 years. Although it had passed only 5.5 years since the latest Miyagi-Oki earthquake on August 2005, the source regions of the past Miyagi-Oki earthquakes again ruptured during the 2011 M9.0 Tohoku-Oki earthquake. Coseismic rupture propagated to Fukushima-Oki, where three M7.3-7.5 earthquakes occurred on 1938. And 30 minutes after the mainshock, the largest aftershock (M7.6) occurred in Ibaraki-Oki, where M<7 earthquakes repeatedly occurred in the past.

Previous two studies based on numerical simulations using the composite law, which is a type of rate- and state-dependent friction law showed contrasting estimations for occurrence of the next (just after the Tohoku earthquake) Miyagi-Oki earthquake. But, both simulations estimated coseismic slip during the mainshock at the correspondent Miyagi-Oki region was much larger than that of seismic and geodetic observations. Then, we numerically simulated cycles for occurrences of seismic and aseismic events along the Japan Trench with the 3D geometry of the Pacific plate using the aging law, which is another type of the friction law. We assumed a slightly stronger frictional heterogeneity at shallower part of the Miyagi-Oki region over a wide range instead to assuming a very strong heterogeneity near the trench as the two previous studies. And we used a small value of seismic radiation damping factor to reproduce shorter propagation time during the M9.0 mainshock.

As a results, we reproduced reasonable coseismic slip at the Miyagi-Oki region, and significantly large coseismic slip along the trench. Models which qualitatively reproduced several observation characteristics showed that time interval between the M˜9 earthquake and the first Miyagi-Oki earthquake after the M˜9 earthquake tend to be shorter than the average recurrence interval observed before the M˜9 earthquake. It corresponds to a previous study of Kato and Yoshida [2011]. Recurrence of M7 class earthquakes after the M9 earthquake should continuously be studied by various models. Observations around M7 class earthquake areas are also important.

Japan Geoscience Union Meeting 2015
(May 24th - 28th at Makuhari, Chiba, Japan)

SSS30-P15 Room:Convention Hall Time:May 25 18:15-19:30

Improvement of an experimental equipment for vibrating a sand-pile -For understanding the mechanism of landslides-

NAKAYAMA, Masayuki[1*] ; KAWAKATA, Hironori[1]

[1]Ritsumeikan Univ.

Landslides have been often triggered by seismic shake and/or rainfall. For example, the 2008 Iwate-Miyagi Nairiku Earthquake induced a massive landslide near Aratozawa Dam in Miyagi prefecture. However, the mechanism of earthquake-induced landslides has not been revealed yet due to the complexity of various factors: geography, geology and groundwater.

Yoshioka (2003) studied the relation between the frequency and the size of avalanches in sand-pile experiments. Nakayama et al. (2014, SSJ) investigated a behavior of a sand-pile when vibration was applied in order to understand the mechanism of the earthquake-induced landslides. They prepared a PET bottle which was cut along its bottom with a cap including a small hole and fixed them on a stand. They dropped dry sand particles in a PET bottle through the small hole and made a sand-pile on an acrylic case on whose bottom a buzzer was attached. Using the buzzer, vibration was input to a sand-pile and recorded the visual behavior of the sand-pile. The size of the sand pile was 60 mm in diameter and 20 mm in height. Two kinds of avalanches were found in their experiments, that is to say, avalanches of the grains of sand independently falling along the sand-pile surface and avalanches of thin sand layers sliding downward along the sand-pile surface. However, such avalanches were not observed on some cases.

In this study, we carried out some more experiments, and went through their experimental condition. We found the spatial variation of amplitudes and dominant frequency of the vibration. In addition, we cannot see the detailed process of avalanches because of lower spatio-temporal resolution.

Then, we try to improve the experimental equipment. For example, we replaced a buzzer to a new one which can change the amplitude and dominant frequency. We changed a shape of the base where we made a sand-pile to reduce spatial variation of the vibration. In addition, we installed a high-speed camera to investigate the process of avalanche in detail.

Acknowledgments:
We are grateful to Dr. I. Doi and Dr. N. Takahashi for their advice and support.

Keywords: lanslide